Lecture 2:

Controlling Ship Dynamics

2.1 Introduction

A ship must be designed to propel through water with maximum efficiency ideally via use of minimum power in waves. Whereas weather phenomena influence ship resistance and associated ship dynamics it is useful to understand the dynamics of calm water resistance. In calm waters a ship experiences a force acting opposite to her direction of motion. This force is the water's resistance to the motion of the ship, which is referred to as total hull resistance (R_T) and is the resistance force used to calculate a ship's effective horsepower. Total hull resistance increases as speed increases (see Figure 2-1). The resistance curve is not linear. Instead it increases more steeply at higher speeds. The hump on the resistance curve shown in Figure 2-1 is a phenomenon common to most ship resistance curves.

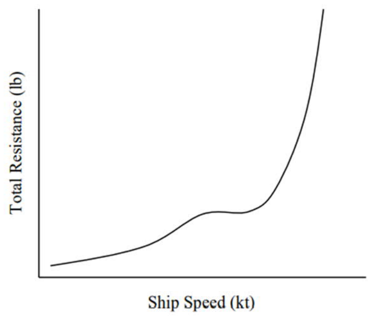

Figure 2-1 *Typical curve of total hull resistance*

A ship's calm water resistance is a function of many factors, including ship speed, hull form (draft, beam, length, wetted surface area), and water temperature. In terms of controlling ship dynamics, it is key to realize that the power required to propel a ship through the water is the product of total hull resistance and ship speed. Thus, engine power increases even more rapidly than resistance. Often, ship power is roughly proportional to the cube of the speed. For example, doubling the speed of a ship from 15 to 30 knots requires $2^3 = 8$ times as much power! For the ship operator planning a voyage, getting from Point A to B in the shortest amount of time (i.e. at high speed) requires a lot more power than traveling the same distance at a slower speed. Naturally, this increase in power is felt directly in the amount of fuel burned during the transit. A ship's fuel consumption curve is similar in shape to its horsepower and total resistance curves. Thus, voyage planning requires careful attention to transit speed and fuel consumption rates to ensure that the ship arrives at its destination with an adequate supply of fuel onboard. Whereas these are items that mostly relate with ship efficiency and marine engineering it is key to realize that resistance and propulsion phenomena interplay in terms of realizing ship dynamic phenomena and their impact on ship safety. This is the reason why in naval architecture we tend to link ship safety and performance in terms of developing rules and standards.

2.2 Key definitions

As a ship moves through the water, the friction of the water acting over the entire wetted surface of the hull causes a net force opposing the ship's motion. This frictional resistance is a function of the hull's wetted surface area, surface roughness, and water viscosity. As water flows along the hull, the laminar flow begins to break down and become chaotic and well mixed. This chaotic behavior is referred to as turbulent flow and the transition from laminar to turbulent flow occurs at the transition point (see Figure 2-1). Turbulent flow is characterized by the development of a layer of water along the hull moving with the ship along its direction of travel. This layer of water is referred to as the "boundary layer". Moving away from the hull, the velocity of water particles in the boundary layer becomes less, until at the outer edge of the boundary layer velocity is nearly that of the surrounding ocean. Formation of the boundary layer begins at the transition point and the thickness of the boundary layer increases along the length of the hull as the flow becomes more and more turbulent. As ship speed increases, the thickness of the boundary layer will increase, and the transition point between laminar and turbulent flow moves closer to the bow, thereby causing an increase in the friction experienced between the ship and surrounding water as speed increases.

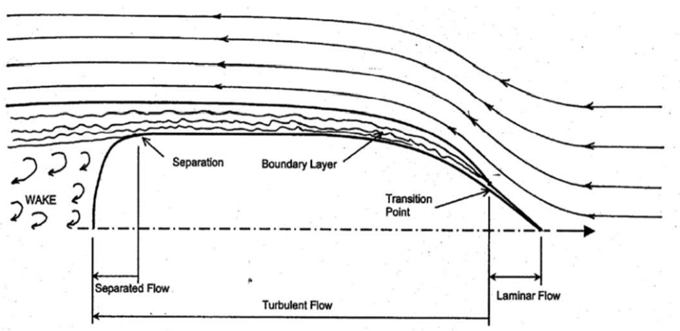

Figure 2-2 *Typical water flow pattern around a ship's hull*

The principle factors affecting total ship resistance are the friction and viscous effects of water acting on the hull, the energy required to create and maintain the ship's characteristic bow and stern waves, and air resistance. Accordingly total resistance (R_T) can be written as:

$$R_T = R_V + R_W + R_{AA} \qquad (2\text{-}1)$$

where: R_T = total hull resistance ; R_V = viscous (friction) resistance ; R_W = wave making resistance ; R_{AA} = air resistance caused by ship moving through calm air. Whereas at low speeds viscous resistance is dominant at high speeds the total resistance curve turns upward dramatically as wave making resistance dominates (see Figure 2-2 and Figure 2-3).

Viscous resistance (R_V) is essentially the result of water rubbing against the ship side. This rubbing is prone to viscosity; a temperature dependent property of a fluid that describes its resistance to flow. Although water has low viscosity, it produces a significant friction force opposing ship motion. Experimental data have shown that water friction can account for up to 85% of a hull's total resistance at low speed ($Fn \leq 0.12$ or speed-to-length ratio less than 0.4 if ship speed is expressed in knots), and 40-50% of resistance for some ships at higher speeds. The influence of frictional resistance depends on the thin water viscosity boundary layer generated around the hull surface as a ship progresses in waves. Friction arises from the shear stresses in the fluid and act tangential to the body. Viscous pressure resistance acts normal to the body. In the forward portion of the hull pressure forces act normal to the surface; however, in the aft portion of the hull the boundary layer reduces the forward acting component of pressure. This reduction in the forward acting component results in a net resistance force due to pressure acting on the hull. This increase in resistance due to pressure is called "*viscous pressure drag*" or "*form drag*", and is sometimes also referred to as the normal component of viscous resistance. The shape of a ship's hull can influence the magnitude of viscous pressure drag. Ships that are short in length with wide beams (a low length to beam ratio) will have greater form drag than those with a larger length to beam ratio. Also, ships that are fuller near the bow (e.g. bulk oil tanker) will have greater form drag than ships with fine bows (e.g. a destroyer or a container ship).

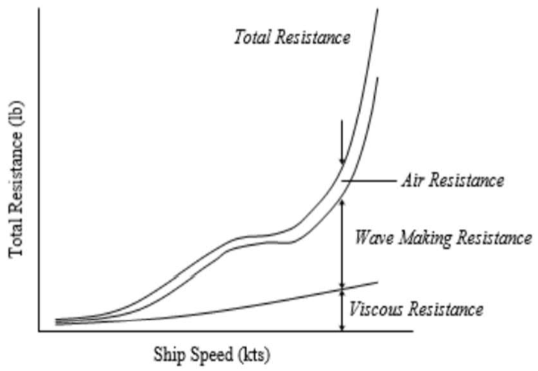

Figure 2-3 Proportional contribution of the components of hull resistance

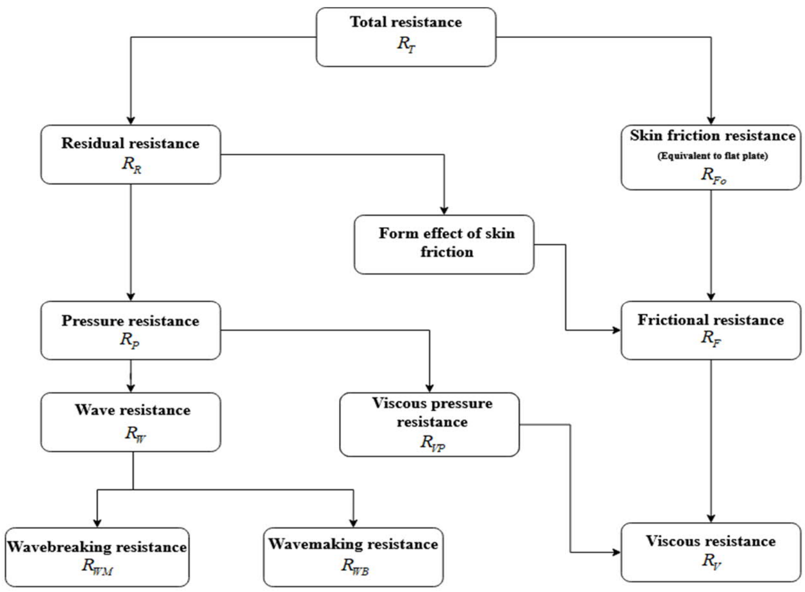

Figure 2-4 *Hydrodynamic resistance components*

Residual resistance (R_R) comprises of the resistance due to waves which are formed by ship motions and eddy making resistance formed in way of the stern and projecting parts such as bossing and bilge keels. Wave resistance relates to the fact that a ship progressing in waves generates a typical wave system leading to energy losses. This wave system is decomposed into primary and secondary systems. The former assumes ideal fluid flow (i.e. no viscosity) leading to pressure distributions. Additionally, at the free surface even with the assumption of the ideal fluid, a typical wave system is generated. The typical wave system comprises transverse and divergent waves (see Figure 2-5). In deep water, waves form a wedge shape known as ''*Kelvin pattern*'' with a half-angle of 19.5º which is independent of the ship actual shape (see Figure 2-5). Sir William Froude (1810-1878) did much of the early research in wave making resistance and his results and conclusions in this field are used to this day.

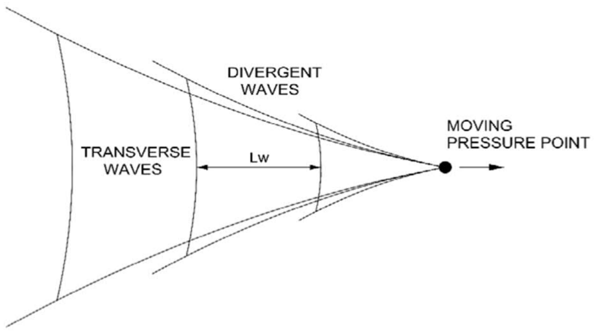

(a) Definitions

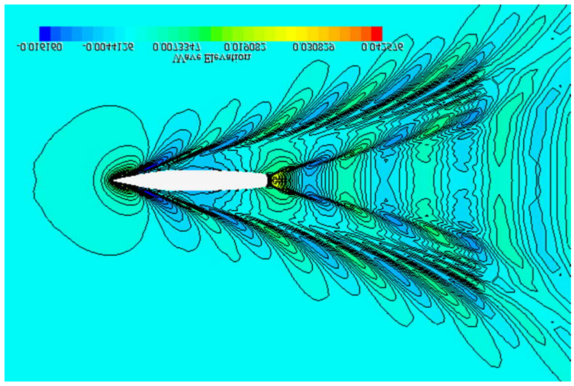

(b) CFD simulation

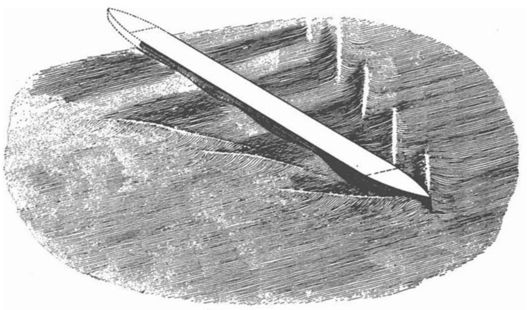

(c) Froude's original sketch of wave patterns

(d) Narrow Kelvin waves by container ship

Figure 2-5 *Idealization of a ship's secondary wave system.*

Air resistance (R_A) acts on portions of the ship above the water. It is the resistance caused by the flow of air over the ship with no wind present. This component of resistance is affected by the shape of the ship above the waterline, the area of the ship exposed to the air, and the ship's speed through the water. Ships with low hulls and small "sail area" or projected area above the waterline will naturally have less air resistance than ships with high hulls and large amounts of sail area. Resistance due to air is typically 4-8% of the total ship resistance, but may be as much as 10% in high sided ships such as aircraft carriers. Attempts have been made reduce air resistance by streamlining hulls and superstructures, however; the power benefits and fuel savings associated with constructing a streamlined ship tend to be overshadowed by construction costs. Wind resistance on a ship is a function of the ship's sail area, wind velocity and direction relative to the ship's direction of travel. For a ship steaming into a 20-knot wind, ship's resistance may be increased by up to 25-30%. Ocean currents can also have a significant impact on a ship's resistance and the power required to maintain a desired speed. Steaming into a current will increase the power required to maintain speed. Added resistance refers to ocean waves caused by wind and storms, and is not to be confused with wave making resistance. Ocean waves cause the ship to expend energy by increasing the wetted surface area of the hull (added viscous resistance), and to expend additional energy by rolling, pitching, and heaving. This component of resistance can be very significant in high sea states. Resistance in shallow waters is caused by (a) the speed up of flow of water around the bottom of the hull leading to increased viscous resistance and (b) the consequent decrease of pressure under the hull, causing the ship to "squat"; thus increasing the wetted surface area and increasing frictional resistance. The waves produced in shallow water tend to be larger than do waves produced in deep water at the same speed. Therefore, the energy required to produce these waves increases, (i.e. wave making resistance increases in shallow water). The net result of traveling in shallow water is that it takes more horsepower (and fuel) to meet required speed.

For slow moving box like ships such as tankers and bulk carriers with high block coefficient the frictional resistance accounts for 70-90% of the total resistance. For faster ocean-going ships that may be slender but have large bow flare and bulky superstructure (e.g. container carriers), the frictional resistance may account for as little as 50%. This is because for box like ocean going ships with high block coefficient it is not possible to make a perfectly streamlined design above the water line as there are difficulties of fabrication and these difficulties are not justified by the amount of resistance reduced. Air resistance normally represents about 2% of the total resistance. However, it may increase up to approx. 10% for ships with large superstructures such as container ships with containers stacked on deck. The value may increase further if wind resistance is considered.

2.3 The dynamics of resistance and thrust

When given the task of designing a ship, the Naval Architect is given a number of design requirements to meet. These include the obvious dimensions such as LPP, Beam and Draft, but also other requirements such as top speed, endurance, operational mission, etc. Some of the more complicated requirements involve maneuverability. These can be split into three broad categories namely (a) general maneuverability in open seas; (b) directional stability/response reflecting (a); (c) low speed maneuverability. These principles are challenged by resistance and thrust dynamics and therefore good design should involve sound understanding of the influence of flow around the hull, the basis of choice of slow and moderate speed steering and maneuvering equipment, and general propulsion dynamics (e.g. propeller rudder interactions). With the later in mind this section explains principles of ship resistance, thrust, their dynamic interactions with direct relevance to ship dynamics.

2.3.1 Ship resistance

Based on the generic definition $Power = Force \times speed$, the ship effective power (i.e. the power the ship would consume if it sails without power) is defined as:

$$P_E = R_T \cdot V_s \tag{2-2}$$

Where R_T is the total water resistance excluding appendage resistance and V_S is the ship speed.

Fluid flow will vary around the hull. Thus, the propeller thrust will depend on the speed of advance (flow speed upstream the propeller) rather than the ship speed. The thrust power will then be defined as:

$$P_T = T \cdot V_A \tag{2-3}$$

Where T is the thrust force generated and V_A is the speed of advance.

The thrust power needed during model tests is usually greater than the total resistance R_T . Thus, the propeller induces additional resistance associated with (a) pressure decreases in way of the aft ship body leading to increase of the inviscid resistance; (b) flow velocity increases around the aft - body that may lead to increases in frictional resistance.

To account for the above, we can combine resistance and thrust together using the so-called thrust deduction factor t defined as:

$$t = 1 - \frac{R_T}{T} \tag{2-4}$$

The resistance that should be equivalent to the propeller thrust is given by the equation:

$$X_{resis\,tan\,ce} = -\frac{R_T}{(1-t)} = -\frac{0.5\rho u^2 S C_T}{(1-t)} \tag{2-5}$$

Where ρ is the water density, u is the longitudinal-component flow velocity, S is the wetted hull surface, and C_T is the total resistance coefficient and this can be in tabular values against Froude number as a result of empirical analysis or model tests.

The speed of advance is generally slower than ship speed because of the effect of the ship's wake on the propeller inflow velocities. This wake is analyzed into mainly three components namely friction, potential and wave wake components. Friction relates with flow velocity speed decreases at the aft ship body's boundary layer and leads to flow separation. Potential does not account for the effects of viscosity in way of free surface and assumes there will be lower velocities at the stagnation points (i.e. in way of the bow and stern of the ship). The wave wake assumes that local velocities around the hull may have adverse or beneficial effects depending on the case. The total wake fraction is then defined by:

$$w = 1 - \frac{V_A}{V_S} \tag{2-6}$$

Self-propulsion CFD simulations can be conducted to evaluate the thrust deduction factor and the wake fraction. (Matusiak 2013) proposed approximate values for wake fraction and thrust deduction factors as shown in Table 2-1.

Table 2-1 Approximate values of the propulsive coefficients (Matusiak 2013)

Item	Single screw vessel	Multi-screw vessel
Wake fraction w	0.25	0.05
Thrust deduction factor t	0.25	0.15

For those cases that the total resistance coefficient is not available the propulsive power P_D may be used to evaluate total resistance as follows:

$$P_D = \frac{P_E}{\eta_D} = \frac{R_T \cdot V_S}{\eta_D}, \; R_T = \frac{P_D \eta_D}{V_s} \tag{2-7}$$

Where η_D is the propulsive efficiency and given by:

$$\eta_D = \eta_o \eta_R \frac{(1-t)}{(1-w)} \tag{2-8}$$

where the open water efficiency $\eta_o = 0.65$ and the relative rotative efficiency $\eta_R = 1$.

2.3.2 Ship thrust

Two models are used to represent the thrust developed by a propeller (see Figure 2-10). Model 1 is preferred for a fixed pitch propeller and comprises the total thrust evaluated from open water characteristics of the propeller (K_T-J curve) as follows:

$$X_{prop} = Z\rho n^2 D^4 K_T \tag{2-9}$$

where Z is the number of propeller blades, n is the propeller revolutions per second, D is the propeller diameter, and K_T is the thrust coefficient. Propeller revolutions should be adjusted for a required ship speed and to satisfy the condition ($X_{prop} = -X_{Re\,sis\,tan\,ce}$), then revolutions are kept constant or to be adjusted to keep the advance coefficient $J = \frac{V_A}{nD}$ constant depending on the type of machinery (Bertram 2012). Model 2 is preferred to controllable pitch propellers. It assumes that the delivered power and the propulsive efficiency are constant. This assumption yields a relationship between the propeller thrust and the ship speed as :

$$X_{prop} = \frac{P_D \eta_o \eta_R}{V(1-w)} \tag{2-10}$$

This model allows good control of the propeller pitch, but it is only optimized for certain design operation conditions and the efficiency losses in other operating conditions are not considered.

(a)Fixed pitch propeller

(b)Controllable pitch propeller

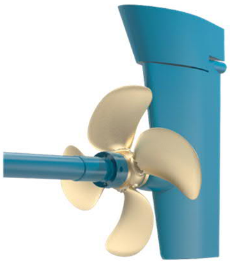

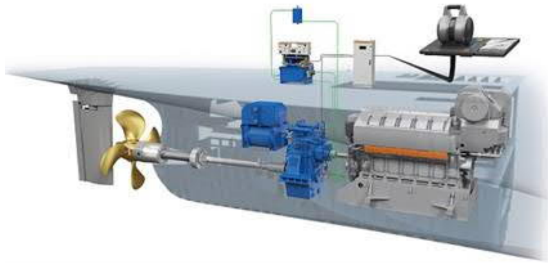

Figure 2-6 Wärtsilä propellers

2.4 Ship rudders

Marine rudders are primary control surfaces with streamlined sections used to steer ships through water. They are designed to give good lift and drag ratio and are of double plate construction (see Figure 2-7Figure 2-7 Figure Rudder concept in ship steering (Shijie et al. 2018)). They are classified based on how close the center of pressure is to the rudder axis as (a) balanced, (b) semi-balanced or (c) unbalanced. Whether a rudder is balanced or not is dependent upon the relationship of the center of pressure of the rudder and the position of the rudder stock. For example. when they are vertically aligned, the rudder is said to be “fully balanced”. This arrangement greatly reduces the torque required by the tiller mechanism to turn the rudder. On the other hand, when the rudder stock is at the leading edge, the rudder is “unbalanced”. This is a common arrangement in merchant ships where rudder forces are not excessive. When no lower pintle is used the rudder is termed as spade. Spade rudders are commonly used in warships (see Figure 2-8).

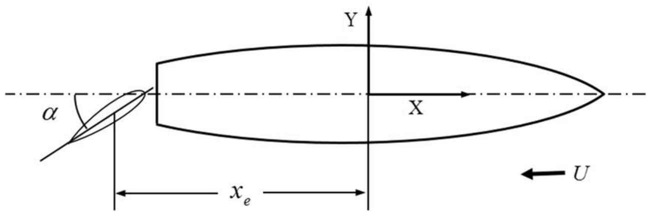

Figure 2-7 Figure Rudder concept in ship steering (Shijie et al. 2018)

Some special rudder types have been developed to increase the rudder lift to drag ratio. A flap rudder has the feature of a flap at the trailing edge of the rudder to improve lift by modifying the aerofoiled shape and to increase the turning angle of the rudder. Another type is the flettner rudder which uses two narrow flaps at the trailing edge. The flaps move to assist the main rudder movement reducing the torque required of the steering gear. Active rudders are spade-type rudders. They include a housing with small electric motor driving small propeller to provide rudder force even when the ship is at rest. Kitchen rudder is very old type with a two-part tube that turns about a vertical axis surrounding the propeller.

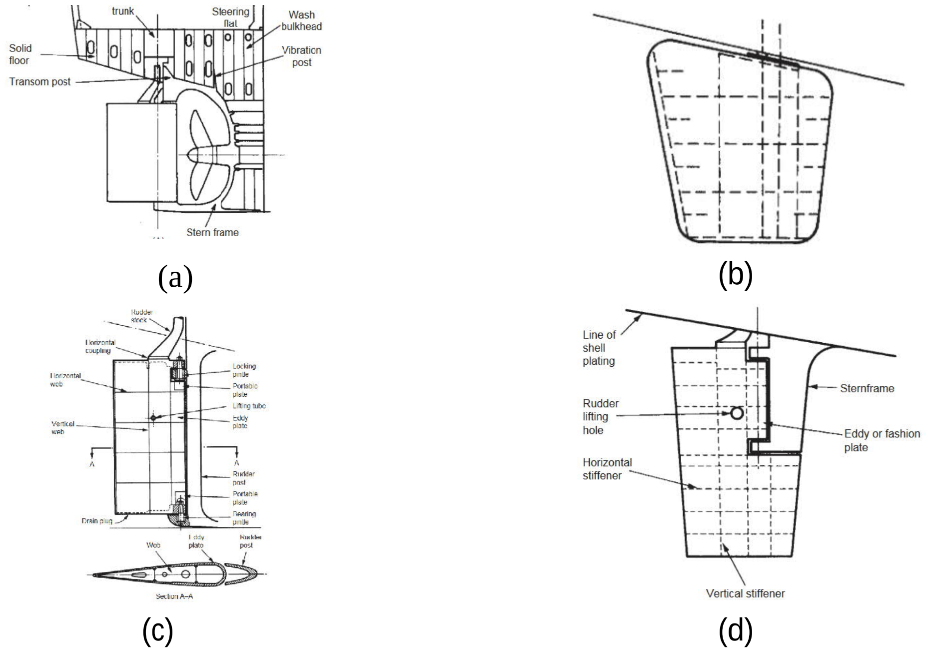

Figure 2-8 Typical rudder types (a) simplex balanced (b) spade balanced (c) unbalanced (d) semi-balanced rudder (Tupper 2013).

It is a common misconception that the rudder turns a ship. In fact, the rudder is analogous to the flaps on an aircraft wing. The rudder causes the ship to orientate itself at an angle of attack to its forward motion. It is the hydrodynamics of the flow past the ship that causes it to turn. The way the rudder affects the forces acting on the flow can be shown using a linear model by set the rudder to an arbitrary angle δ . This action develops a horizontal force is given as:

$$Y_R = Y_\delta \delta \tag{2-11}$$

where $Y_\delta = \partial Y / \partial \delta$ is a hydrodynamic derivative in way of the axis of reference (Matusiak 2013). This is followed by a negative turning moment $N_\delta \delta$. This results in a turning motion of the ship to an angle β and amplified by a turning moment $N_v v$ as the ship is positioned in an inclined flow (see Figure 2-9).

(a) Inflow rudder velocity and rudder forces (Matusiak, 2013) (b)Stages of ship's turn

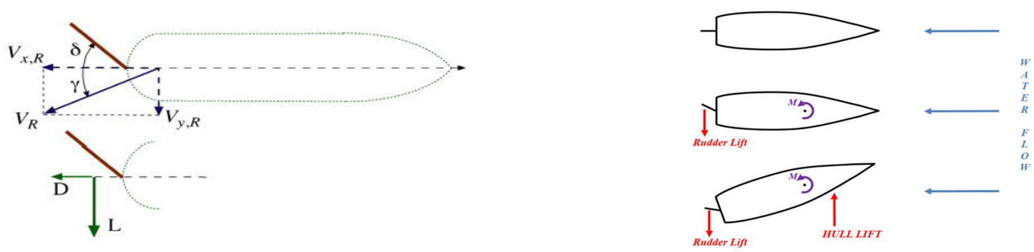

Figure 2-9 Rudder Dynamics

There are two main realistic ways to evaluate the rudder forces. The first is known as the non-linear maneuvering model that utilizes the hull forces as a function of the rudder angle:

$$
\begin{aligned}
X &= X_{\dot{u}}\dot{u} + X_u u + X_{uu}u^2 + X_{uuu}u^3 + X_{vv}v^2 + X_{rr}r^2 + X_{\delta\delta}\delta^2 + X_{vr}vr \\
&+X_{v\delta}v\delta + X_{r\delta}r\delta + X_{vvu}v^2u + X_{rru}r^2u + X_{\delta\delta u}\delta^2u + X_{r\delta u}r\delta u + X_{rvu}rvu \\
&+X_{v\delta u}v\delta u + X_{r\delta v}r\delta v
\end{aligned}
\tag{2-12}
$$

$$
\begin{aligned}
Y &= Y_{uu}u^2 + Y_{\dot{v}}\dot{v} + Y_{\dot{r}}\dot{r} + Y_v v + Y_r r + Y_\delta\delta + Y_{\delta u}\delta u + Y_{vu}vu + Y_{ru}ru + Y_{vuu}vu^2 \\
&+Y_{ruu}ru^2 + Y_{\delta uu}\delta u^2 + Y_{vvv}u^3 + Y_{rrr}r^3 + Y_{\delta\delta\delta}\delta^3 + Y_{rr\delta}r^2\delta + Y_{vrr}vr^2 + Y_{rvv}rv^2 \\
&+Y_{\delta vv}\delta v^2 + Y_{vr\delta}vr\delta + Y_{\delta\delta r}\delta^2 r + Y_{\delta\delta v}\delta^2 v
\end{aligned}
\tag{2-13}
$$

$$
\begin{aligned}
N &= N_{uu}u^2 + N_{\dot{v}}\dot{v} + N_{\dot{r}}\dot{r} + N_v v + N_r r + N_\delta\delta + N_{\delta u}\delta u + N_{vu}vu + N_{ru}ru \\
&+N_{vuu}vu^2 + N_{ruu}ru^2 + N_{\delta uu}\delta u^2 + N_{vvv}v^3 + N_{rrr}r^3 + N_{\delta\delta\delta}\delta^3 + N_{rr\delta}r^2\delta \\
&+N_{vrr}vr^2 + N_{rvv}rv^2 + N_{\delta vv}\delta v^2 + N_{rv\delta}vr\delta + N_{\delta\delta r}\delta^2 r + N_{\delta\delta v}\delta^2 v
\end{aligned}
\tag{2-14}
$$

Another model to be used is the modular model in which the flow in way of the rudder is modelled mathematically. Since the inflow velocity to rudder is influenced by yaw and sway motion of the ship it influences the propeller slipstream flow and the flow velocity due to wave action. The angle of attack of the flow is not the same as the rudder angle. Consequently, the drag and lift forces depend on the flow velocity in way of the rudder defined as:

$$
\begin{Bmatrix} V_{x,R} \\ V_{y,R} \\ V_{z,R} \end{Bmatrix} = \begin{Bmatrix} V_x - V_{x,wave} \\ -v + V_{y,wave} \\ -w + V_{z,wave} \end{Bmatrix} - \begin{Bmatrix} -i & j & k \\ p & q & r \\ x_R & y_R & z_R \end{Bmatrix} \rightarrow \begin{matrix} V_{x,R} = V_x - V_{x,wave} - qz_R + ry_R \\ V_{y,R} = -v + V_{y,wave} - rx_R + pz_R \\ V_{z,R} = -w + V_{z,wave} - py_R + qx_R \end{matrix}
\tag{2-15}
$$

In the above equation V_x is the longitudinal (x-component) of flow velocity along the propeller slipstream. The subscript ‘‘*wave*’’ is referred to the flow velocities due to the contribution of wave action; (x_R, y_R, z_R) represent the positions of the rudder in the body-fixed coordinate system (see Figure 1-2 and (Taimuri et al. 2020)). V_R is the rudder flow velocity vector with angle of attack $\alpha = \delta + \gamma$ (see Figure 2-9).

A typical ship’s rudder is limited to a range of angles up to about ± 35°. This is because at greater angles than these the rudder is likely to stall. Figure 2-10 shows the development of stall as rudder angle increases. Lift and drag forces are defined as :

$$L = \frac{1}{2}\rho C_L A_R V_R^2 \tag{2-16}$$

$$D = \frac{1}{2}\rho C_D A_R V_R^2 \tag{2-17}$$

where A_R is the projected area of the side view of the rudder.

And the corresponding lift and drag coefficients become:

$$C_L = \frac{2\pi\Lambda(\Lambda+1)}{(\Lambda+2)^2} sin(\delta+\gamma),\ C_D = 1.1\frac{C_L^2}{\pi\Lambda} + C_{D0} \tag{2-18}$$

where $\Lambda = b^2 / A_R$ is the aspect ratio, and b is the rudder length (see Figure 2-9).

The viscous drag coefficient and it can be calculated according to the ITTC 1957 (Morrall 1970) frictional resistance coefficient and the form factor of the rudder:

$$C_{D0} = 2.5C_F = 2.5\frac{0.075}{(log\,Rn-2)^2}$$

$$Rn = \frac{V_R c}{v} \tag{2-19}$$

where Rn is Reynold's number, c is the mean value of the rudder cord and v is the kinematic viscosity.

At small angles, rudder lift is created due to the difference in flow rate across the port and starboard sides of the rudder. However, as rudder angle increases, the amount of flow separation increases until a full stall occurs at 45º degrees. The amount of lift achieved by the rudder reduces significantly after a stall and is matched by a rapid increase in drag. Consequently, rudder angle is limited to values less than the stall angle.

(a) Rudder Flow Patterns at Increasing Rudder Angle (b) Lift versus rudder angle

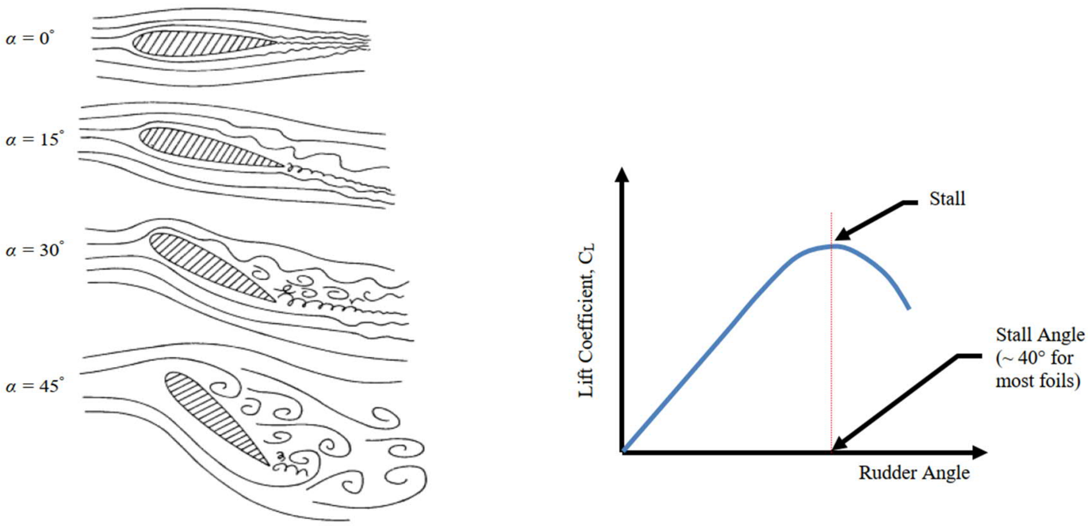

Figure 2-10 Rudder flow patterns at increasing rudder angle

Note that we assume that the rudder is positioned directly in the propeller slipstream. Accordingly, the rudder forces are higher than the ones generated by a rudder placed outside the propeller. Since there a distance even small between the propeller and the rudder, this results in reduction of the axial velocity of the slipstream V_x when reaches the rudder. The velocity at the rudder can be then represented as a function of the velocity far downstream the propeller, the radius of the flow far downstream the propeller, and the radius of the slipstream at the rudder:

$$\frac{V_x}{V_\infty} = \left(\frac{r_\infty}{r}\right)^2$$

$$\frac{r}{r_0} = \frac{0.14(r_\infty / r_0)^3 + (r_\infty / r_0)(r_\infty / r_0)^{1.5}}{0.14(r_\infty / r_0)^3 + (r_\infty / r_0)^{1.5}} \qquad (2\text{-}20)$$

where V_∞ is the mean flow velocity far downstream the propeller, r_∞ is the radius of the slipstream far behind the propeller, r is the slipstream radius at the rudder, r_0 is the propeller radius. By assuming the ideal propulsor model, the axial mean velocity and the slipstream radius far behind the propeller can be approximated using:

$$V_\infty = V_A\sqrt{1 + C_T} \;\; \text{for } C_T = \frac{Thrust}{0.5\rho V_A^2 \pi D^2/4} = \frac{8}{\pi}\frac{K_T}{J^2} \text{ while } r_\infty = r_0\sqrt{\frac{1}{2}\left(1 + \frac{V_A}{V_\infty}\right)} \qquad (2\text{-}21)$$

C_T is the thrust loading coefficient, and D is the propeller diameter.

2.5 The influence of slow speed maneuverability

Safe and sustainable operations require that a ship maintains sufficient and independent directional control in restricted waters such as in ports and channels and in various environmental conditions. Such maneuvers take place at low speeds where rudders are limited in terms of their effectiveness due to lack of flow across their surface. There are several modifications made to classic propulsion systems and equipment that have been improved to improve this situation namely:

- The rudder is often positioned directly upon the control surface. A skilled helmsman can then combine the throttle control and rudder angle to vector thrust laterally and create a larger turning moment with minimal advance and transfer
- The presence of two propellers working in unison (twin propulsion system) offers the opportunity to apply a ‘‘twist manouvre’’; i.e. turn one propeller in reverse direction and the other in forward direction; thus create large turning moments with hardly any forward motion
- Implement lateral thrust units at the bow and the stern. Bow thrusters are enclosed in transverse tubes/tunnels (see Figure 2-11) known as suction tunnels. In typical thruster models the suction tunnel length is usually 2-3 times the diameter of the unit. The average bow thruster power in ferries is 0.54kW/m2 (total bow thruster power/projected windage area), varying up to 0.96 kW/m^2. Nowadays, the tendency seems to be towards 0.6-0.8 kW/m^2. Stern thrusters are dimensioned at 0.2-0.25 kW/m^2 (Watsila 2020).
- Implement rotational thrusters also known as azimuth propulsion systems that may rotate up to 360^0 (see Figure 2-12). These are shaft-less electric propulsion systems prone to minimal noise and vibration. They are more efficient than propellers in oblique inflow conditions. A simple model of the forces acting on the azimuth propellers is outlined on Figure 2-12b. In this model that the rate of change of the pod is small so that we deal with it in a quasi-stationary approach in incompressible flow. Note that we also do not deal with the forces acting on the pods but the propeller disk (forces acting on the pod and the strut are disregarded).

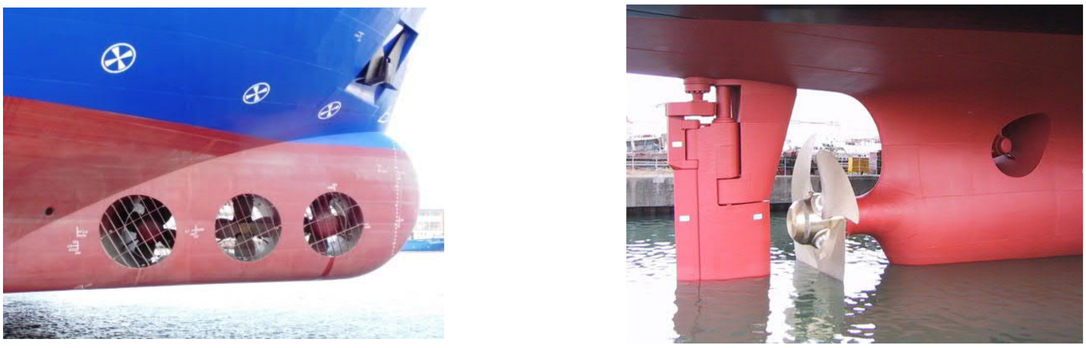

(a) (b)

Figure 2-11 (a) Bow thrusters (b) stern thruster (www.kamome-propeller.co.jp & www.wikipedia.org)

(a) Typical rotational thruster design by Kvaerner Masa (Finland)

(b)Oblique flow kinematics for a thruster unit (Matusiak 2013)

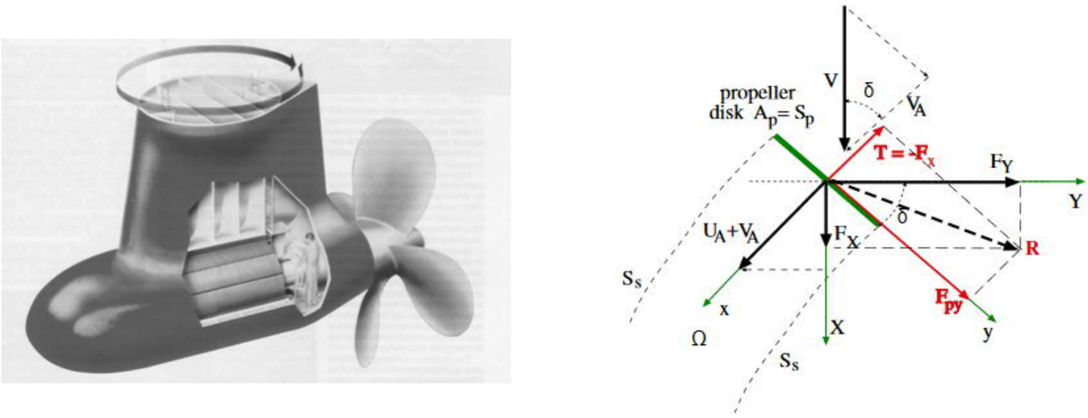

Figure 2-12 Rotational thruster dynamics

In such conditions the forces acting on the propeller in oblique flow are changing axially and radially. Accordingly, an in-plane force will be developed in addition to the axial component and the magnitudes of corresponding unsteady forces and moments amplify. The governing equation used to derive these forces is the momentum equation. This equation in its integral form states that : ''the rate of change of momentum in an arbitrary domain is equal to the body forces and the surface forces acting on the domain boundaries''. Thus:

$$\frac{D}{Dt}\int_{\Omega}(\rho v_i)d\Omega = \frac{\partial}{\partial t}\int_{\Omega}\rho v_i d\Omega + \int_{S}\rho v_i(\vec{v}\cdot\vec{n})dS = \int_{S} q_i dS + \int_{\Omega} F_i d\Omega \qquad (2\text{-}22)$$

where Ω denotes the arbitrary control volume, $\frac{\partial}{\partial t}\int_{\Omega}\rho v_i d\Omega$ is the rate of change of momentum in the control volume, $\int_{S}\rho v_i(\vec{v}\cdot\vec{n})dS$ represents the total momentum flux outflow the domain/control volume, $\int_{S} q_i dS$ are the surface forces acting on the boundaries of the domain, and $\int_{\Omega} F_i d\Omega$ are the body in the domain. The body forces are assumed to be small and negligible. The surface forces at any boundary are disregarded unless for the surface of the propeller disk S_P (see Figure 2-12 (b)). The momentum equation is accordingly reduced to:

$$\int_{A_P} q_i dS = -\int_{S_p} \rho v_i (\vec{v} \cdot \vec{n}) dS = \vec{R} \qquad (2\text{-}23)$$

where A_p is the propeller disk area. In the previous equation, we get an important conclusion that the total momentum flux acting on the propeller disk is equal to the total surface forces $\vec{R}$ acting on it. The in-plane component of the surface forces acting on the propeller disk is given by:

$$F_{Py} = \rho A_P (V_A + U_A) V_S \sin\delta \qquad (2\text{-}24)$$

U_A is the propeller induced velocity in the propeller plane and given as:

$$U_A = \frac{1}{2} V_A \left(-1 + \sqrt{1 + C_T}\right) \qquad (2\text{-}25)$$

Since we have two coordinate systems; the ship fixed coordinate system (*X*-*Y*) and the one moves with the pod (x-y), the X-component force drive the ship in ahead/astern direction, and the *Y*-component force act instead of a rudder are given in terms of the propeller thrust T and the in-plane force F_{Py} :

$$F_x = T\, cos\,\delta - F_{py}\, sin\,\delta \qquad (2\text{-}26)$$

$$F_y = T\, sin\,\delta + F_{py}\, cos\,\delta \qquad (2\text{-}27)$$

Another difference between conventional propellers and azimuthing ones is the difference in the stopping action; the later have quite faster stopping than the former.

2.6 Stabilisation systems

In this section we discuss the influence of hull form on ship motions and within the context of preliminary ship design, i.e. without accounting for multi-objective procedures (Papanikolaou et al. 2010) that could lead to more complex yet optimized design choices. Within this context conventional ship stabilisation systems may be used to control roll motions. Bilge keels are the most conventional passive system for roll motion reduction. They are plates projecting out from the turn of bilge and extending over half to *2/3* of the ship's length. The projection out from the bilge of keel should not be too large to avoid damage or collision especially in restricted waters. However, they may be extended enough to penetrate the boundary layer. The movement of a body of water with the ship due to the existence of the bilge keel may lead to reduction in the amplitude of roll and increase in the roll period. They work by generating drag forces which oppose the rolling motion of the ship. Thus, their effects are prominent at higher speeds. The advantage of bilge keels is that they are simple, inexpensive and can be maintained as part of the hull maintenance procedure. Their disadvantage is that they increase the resistance of the ship. Passive tanks are stabilizers that involve a sloshing liquid used to produce damping and restoring forces. They work by shifting weight of the liquid so that it exerts a roll moment on the ship and (by suitable design) this can be arranged to damp roll motion. Accordingly the natural frequency of the tank should be equal or near the ship's natural frequency and to achieve this the tank is tuned by adjusting the amount of liquid in the tank or by the design of a baffle. A passive tank system is good choice if space and weight requirements are not of major concern. There are no moving parts and it requires little maintenance. U shaped passive tanks include water that moves and helps the ship stabilize as she inclines. A drawback for such system is that the tank can be adjusted to only one frequency corresponding to the roll natural period at which large motion amplitudes occur. The water free surface in the tank may affect stability and must be allowed for. Active tanks are similar in principle to passive tanks, but the movement of water is controlled by pumps or by air pressure above the water surface instead of the passive action of water. They can be two separate tanks on both sides of the ship or connected with lower limb. The system can deal with more than one frequency and in similar fashion to the passive system it can stabilize at zero ship speed. There are no projections outside the hull. Active Fins system is the most popular active system. In this stabilisation model one or more pairs of fins are fitted on both sides of the ship. They move with the aid of an actuating system in response to signals based on gyroscopic measurements of roll motions. The fin may move totally or partly. The fins may permanently protrude from the bilge or may, at the expense of some complication, be retractable. The lift force on the fin is proportional to the square of the ship's speed. At low speed they will have little effect although the control system can adjust the amplitude of the fin movement to take account of speed, using larger fin angles at low speed. Active T-foils are the same on shape and principle to active fins. however, they have active flaps that can be adjusted to reduce roll as well as pitch motions and may reduce heave. They might be seen common in catamaran ships as they are relatively shorter than displacement ships and motion reduction in this type of ships is demanding.

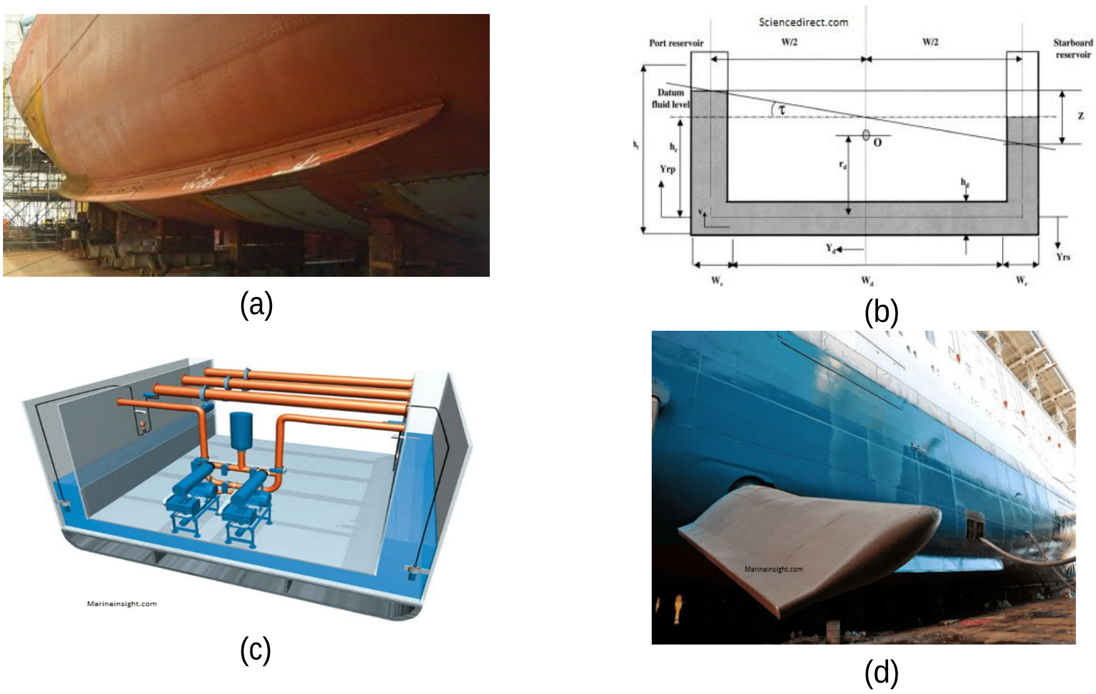

Figure 2-13 (a) Bilge keel (b) Passive rolling tank (c) active rolling tank (d) active fins

2.7 References

Bertram, Volker. 2012. *Practical ship hydrodynamics*: Elsevier.

Matusiak, Jerzy. 2013. *Dynamics of a Rigid Ship*. Espoo, Finland: Aalto University.

Morrall, A. 1970. "1957 ITTC model ship correlation line values of frictional resistance coefficient." *National Physical Laboratory, NPL, Ship Division, Ship Report 142*.

Papanikolaou, Apostolos, George Zaraphonitis, Evangelos Boulougouris, Uwe Langbecker, Sven Matho, and Pierre Sames. 2010. "Multi-objective optimization of oil tanker design." *Journal of marine science technology* 15 (4):359-373.

Shijie, Lin, Ma Yong, Zheng Weitao, Zhang Song, Lei Xiaoshan, and He Yangying. 2018. *Investigation on Rudder Hydrodynamics for 470 Class Yacht*. Queensland, Australia,: 12th Conference of the International Sports Engineering Association.

Taimuri, Ghalib, Jerzy Matusiak, Tommi Mikkola, Pentti Kujala, and Spyros Hirdaris. 2020. "A 6-DoF maneuvering model for the rapid estimation of hydrodynamic actions in deep and shallow waters." *Ocean Engineering* 218:108103.

Tupper, Eric Charles. 2013. *Introduction to naval architecture*: Butterworth-Heinemann.

Watsila. 2020. "Encyclopedia of Marine Technology."